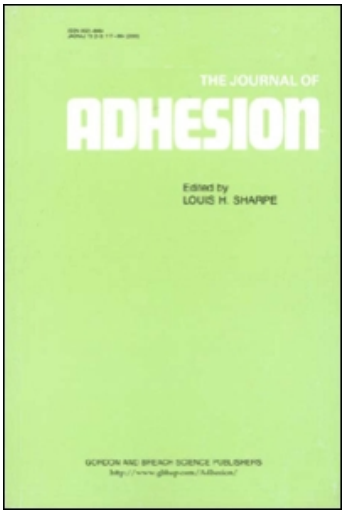

The Journal of Adhesion
Publication details, including instructions for authors and subscription information:
http://www.informaworld.com/smpp/title~content=t713453635

Surface Roughness and Particle Adhesion

H. A. Mizes[a]
[a] Xerox Webster Research Center, Webster, NY, USA

To cite this Article Mizes, H. A.(1995) 'Surface Roughness and Particle Adhesion', The Journal of Adhesion, 51: 1, 155 — 165
To link to this Article: DOI: 10.1080/00218469508009995
URL: http://dx.doi.org/10.1080/00218469508009995

J. Adhesion, 1995, Vol. 51, pp. 155–165
Reprints available directly from the publisher
Photocopying permitted by license only

Surface Roughness and Particle Adhesion*

H. A. MIZES

Xerox Webster Research Center, 800 Phillips Rd. 114-23D, Webster, NY 14580, USA

(Received May 4, 1994; in final form September 6, 1994)

One of the important mechanisms affecting particle adhesion is the geometry of the contact between the particle and the surface. Atomic force microscopy can measure both this geometry and the particle adhesion. The positional dependence of adhesion of a point probe to a variety of rough surfaces has been measured. The Derjaguin approximation predicts that the adhesion fluctuations are proportional to the surface curvature fluctuations, if the adhesion is dominated by long range forces. Atomic force microscopy adhesion maps have directly verified this linearity.

KEY WORDS adhesion; particle; xerography; atomic force microscopy; loading curve; surface roughness; surface curvature; Derjaguin approximation.

1. INTRODUCTION

The xerographic process requires the transfer of toner particles from one surface to another.[1-2] As shown in Figure 1, this is accomplished by charging the particles using contact electrification and applying an electric field to move the particles. Adhesion of the particle to the surface opposes the electrostatic transfer. An electric field strong enough to overcome this adhesion must be applied. If the surface has adhesion inhomogeneities, then the critical field for particle transfer will depend on the particle location. When an insufficient field is applied, some particles will remain on the original surface. The incomplete transfer of particles will affect the final image quality. Image density fluctuations may occur for black and white images, and color shifts in color images.

Three sources of the adhesion variation are illustrated in Figure 1. For rough surfaces, particles that fit snugly into pits or grooves will feel a stronger attraction to the surface, and particles that sit atop bumps or ridges will fell a weaker adhesion. Surface inhomogeneities arising either from the surface material or from adsorbates may cause particles to adhere more strongly to some regions over others. The particles also will vary in size and will have different charges and, therfore, each can feel a different attraction to the same surface. All of these effects can be directly probed with atomic force microscopy (AFM) on a local scale.

* Presented at the Seventeenth Annual Meeting of The Adhesion Society, Inc., in Orlando, Florida, U.S.A., February 21–23, 1994.

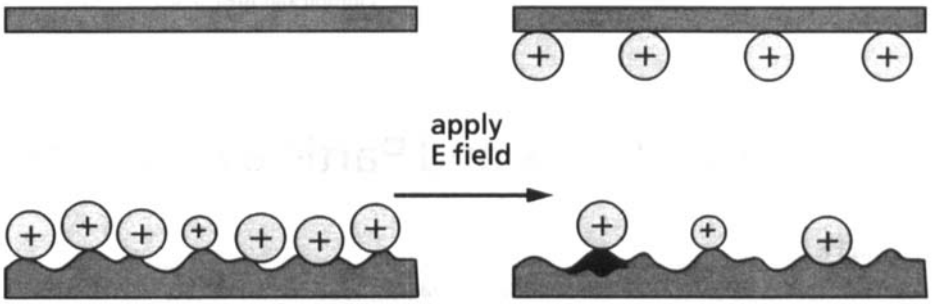

FIGURE 1 Schematic of the transfer of particles that occurs at many steps in the xerographic process. Variations in the particle and the surface can prevent their removal with an electric field. From the left, the first particle remains because of a sticky area on the surface, the second because it is smaller and less of an electrostatic force acts on it, and the third because it fits into a pit which increases the van der Waals attractive forces.

In an earlier work, we quantified how the application of an electric field can change the adhesion of polymer particles to a surface,[3] and how adhesion inhomogeneities on a length scale that affect particle adhesion can be measured with AFM.[4] In this paper, we show how surface roughness modifies particle adhesion. A comparison of AFM adhesion maps and topography maps illustrate the relationship between adhesion and surface topography. A more quantitative analysis of AFM adhesion maps allows a direct verification of the Derjaguin approximation for the adhesion between two curved surfaces.

2. FORCE CURVE MEASUREMENT WITH ATOMIC FORCE MICROSCOPY

AFM can determine the adhesion of individual particles by directly measuring the force required to remove them from a surface. The small particle is attached to a microfabricated cantilever of silicon nitride and the cantilever is brought near the surface. The surface is attached to a piezoelectric transducer that can move in three dimensions with better than 1 nm precision. The adhesion is measured by taking a force curve. We used a Park Scientific Instruments AFM and wrote our own software to capture the force curves.

A typical force curve is shown in Figure 2. For large separations the cantilever does not move as the surface is brought closer to the particle. When the surface is within a few tens of nanometers from the probe, the particle jumps to the surface. Further sample motion in the same direction bends the cantilever backwards and increases the loading force of the particle against the surface.

When the piezoelectric is contracted and the surface moves downward, the probe adheres to the surface causing the cantilever to bend down. The probe continues to adhere until the bent cantilever generates enough force to pull the particle off the surface. The cantilever then springs back to its resting position.

This technique allows the measurement of quite small forces. The cantilever spring is only 0.6 μm thick and, depending on the geometry, can have force constants between

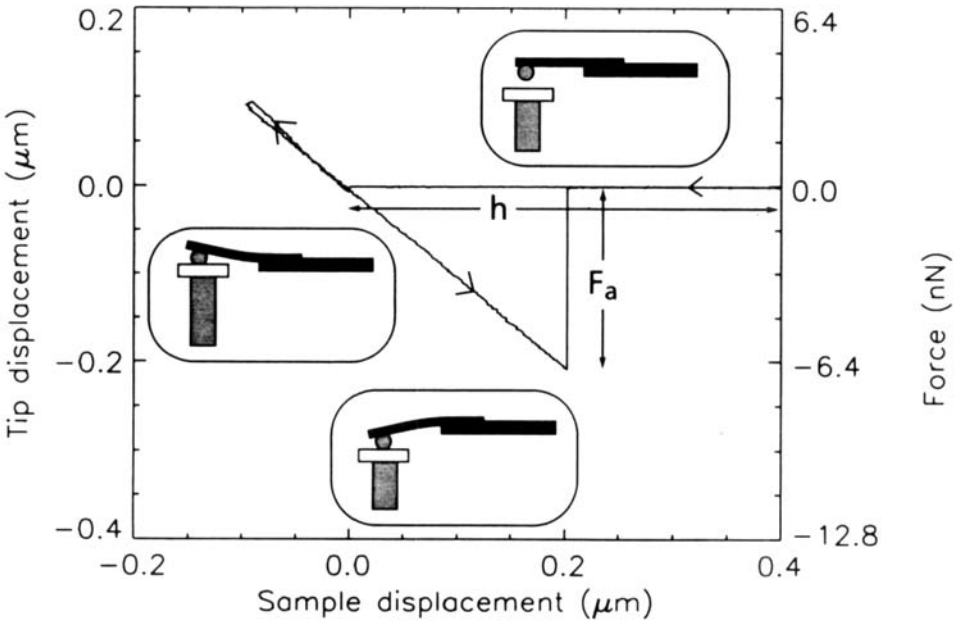

FIGURE 2 A loading curve measured with the AFM. The arrows on the curve indicate the order in which the data are collected. The insets show the relative position of the probe and the surface at different points in the loading curve.

~ 0.04 N/m to ~ 0.4 N/m. The displacement of the cantilever is detected optically[5] with a precision of about 0.1 nm. This leads to a minimum force sensitivity of 0.003 nN and, at the piezoelectric's maximum extension of 7 μm, a maximum detectable force of 3000 nN.

From a loading curve, one can extract simultaneously the removal force of the particle from the surface and the relative height. The removal force is proportional to the maximum downward displacement of the cantilever. The constant of proportionality or the spring constant, k, of the cantilever is calculated from the geometry of the cantilever and the elastic modulus of SiN.

Figure 3(a) shows a particle that has been attached to a cantilever and measured with AFM. In general, both the particle and the surface will have a surface roughness and material inhomogeneities that will affect the adhesion. The roughness of the particle can lead to the large differences in expected values of adhesion and model theories.[6] In order to simplify the measurements, integrated pyramidal tips as shown in Figure 3(b) have been used in this work to probe the adhesion. These tips are deposited during microfabrication of the cantilever. The point of the tip has a radius of curvature less than 30 nm.[7] The pyramid should have only one contact point with surfaces that are studied and be homogeneous over the area of the contact. The pyramid guarantees that only the variations in the sample are driving the changes in adhesion.

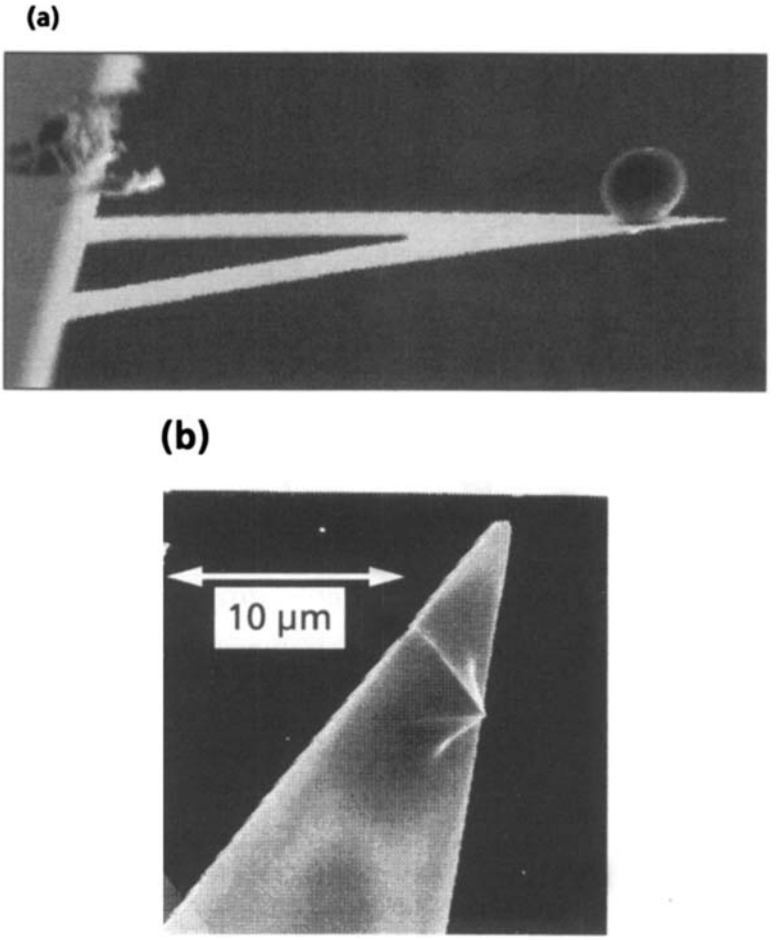

FIGURE 3 (a) Scanning electron micrograph of a 22 μm latex particle attached to a silicon nitride cantilever. (b) Scanning electron micrograph of an integrated pyramidal tip.

3. TOPOGRAPHIC DEPENDENCE OF ADHESION

The piezoelectric transfer to which the particle is attached can move not only up and down, but also laterally. Loading curves can then be taken in a grid pattern over different areas of the surface. From the set of loading curves two images can be generated: a topography map from the collection of sample heights as a function of position, and an adhesion map from the collection of adhesion values as a function of position.

Figure 4 shows the simultaneously-obtained adhesion and topography map of a polycarbonate surface. The image was taken over a region of the surface that was scratched. In the topographic map the scratch is observed running from the bottom to

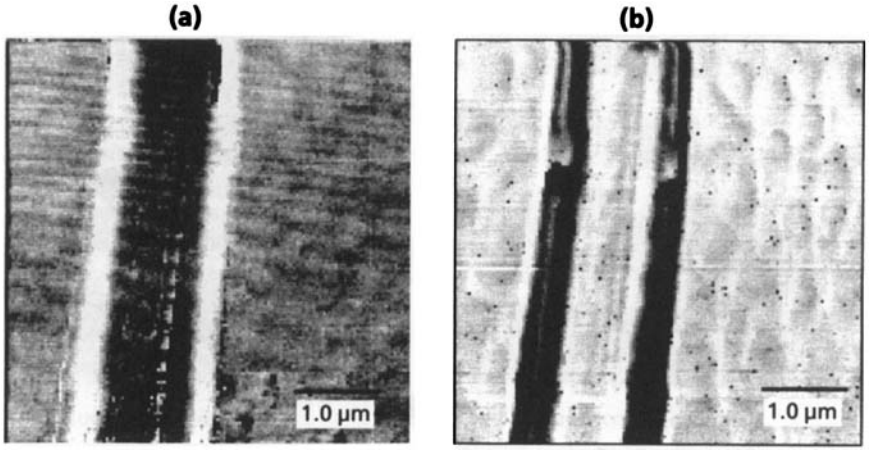

FIGURE 4 (a) Topography map of a scratch in polycarbonate. The height difference between black and white is 0.2 μm, with white being higher. (b) Adhesion map of a scratch in polycarbonate. The adhesion difference between black and white is 35 nN, with white corresponding to larger values of adhesion.

the top of the image. The scratch consists of a groove in the center with a ridge of material on either side of it. The adhesion map shows that the adhesion of the pyramial probe is lower to the top of the ridges of the scratch. This can qualitatively be understood from the geometry of the system. When the pyramidal tip is touching the top of a ridge the two surfaces are curved away from each other. The attraction between the surfaces should then be less than when the tip is over a flat region of the surface when they are in closer proximity over a larger area.

Figure 5(a) shows the simultaneously-obtained adhesion and topography map of the surface of Tedlar®/polycarbonate blend. Many observations of this surface show that if any phase separation of the polymers is occurring it is not affecting the adhesion. The adhesion was seen to depend only on the surface topography. In this particular image, a bump is seen in the topography map, indicated by the arrow. The bumps correspond to low adhesion values in the adhesion map. In addition, over what appear to be flat areas of the surface in topography, there are still variations in adhesion seen in the adhesion map. These variations occur on the same length scale as bumps in the film, so it is reasonable to assume that the adhesion is dominated by the topography that is not resolved in the topography map.

A more quantitative comparison of the topography and adhesion can be made by examining the bumps in more detail. Figure 5(b) shows a contour map of both topography and adhesion for the center bump of Figure 5(a). The bump is seen to be 160 nm high. The adhesion contour map has a minimum value of less than 5 nN occurring near the top of the topography bump. The adhesion over the flat areas away from the bump is approximately 20 nN. There is an incomplete ring around the bump consisting of higher values of adhesion between 25 nN and 30 nN. These are the regions on the side of the bump that curve in the same direction as the tip. The tip fits more snugly into these regions and, thus, gives the higher value of adhesion.

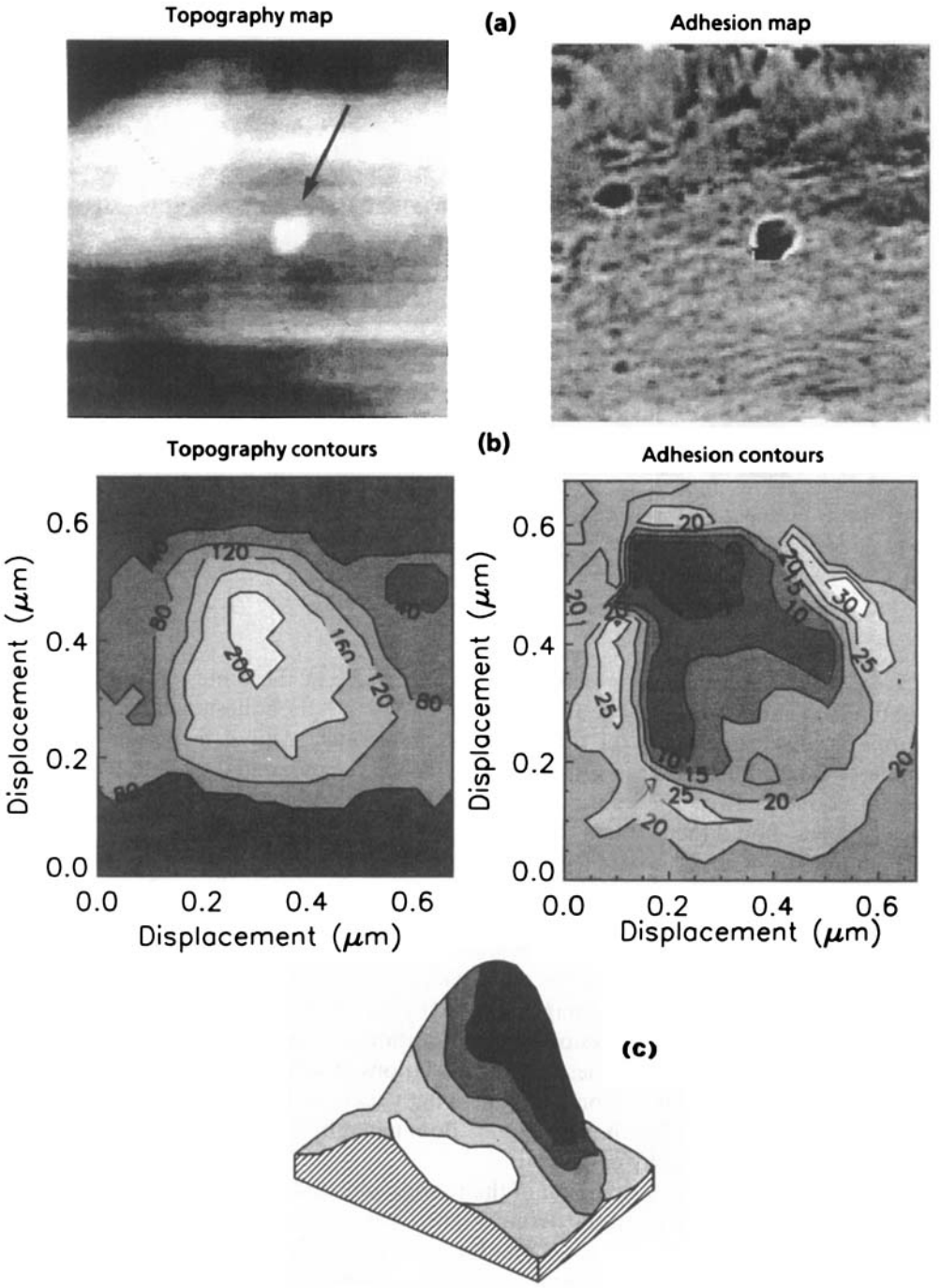

FIGURE 5 (a) Topography and adhesion map of Tedlar®/polycarbonate blend. In the topography map white is higher , and in the adhesion map, white is stronger adhesion. (b) Contour map of the bump indicated by the arrow. The units of the topography map contours are nm, and of the adhesion map contours are nN. (c) 4-dimensional representation of the topography of the bump and adhesion to the bump. The gray levels are the same as in the adhesion map of (b).

Adhesion and topography can be displayed simultaneously for the bump. This is shown in Figure 5(c). The data have been smoothed using a Fourier transform with highpass spatial filtering. The topography of the surface is displayed in perspective and the lightness of the surface increases with the magnitude of the adhesion. The minimum value of adhesion is slightly off center from the top of the bump. This offset is probably due to the tip's asymmetry. The end of the tip is probably better represented by tilted ellipsoid rather than by a sphere.

The force holding the particle to the surface depends on long-range interactions. For Van der Waals forces between two macroscopic bodies, the approximation is made that only 2-body interactions dominate. The total force between the two bodies is determined by integrating over the volumes of both bodies.

The Derjaguin approximation to the interaction force looks at the case where the separation between two bodies is much less than the size of the bodies. For adhesion between a particle and a surface, where they are in intimate contact, this is certainly the case. Then the adhesion is dominated by the curvature of the two surfaces about the point of contact. For two spheres, the force as a function of the distance of separation is given by[8]

$$F(D) = 2\pi\left(\frac{R_t R_s}{R_t + R_s}\right) W(D) \tag{1}$$

where R_t and R_s are the radii of curvature the two spheres, and D is the distance of separation. $W(D)$ is the energy per unit area of two flat surfaces at the same separation, D. The approximation holds for arbitrarily-shaped bodies that can be approximated by spheres at their point of contact. The Derjaguin approximation, thus, is an expression that separates the geometric effects that control adhesion from all the other material effects.

For our purposes, the Derjaguin approximation becomes clearer if it is written in terms of the curvatures of the surfaces, which are the inverse of their radii of curvature. If we take $C_t = 1/R_t$ to be the curvature of the tip, $C_s = 1/R_s$ to be the curvature of the surface at the point of contact, and set $D = 0$, then

$$F_R = W\left(\frac{1}{C_t + C_s}\right) \tag{2}$$

The Derjaguin approximation gives a more quantitative explanation for the results in Figure 5. On the flat regions of the surface $C_s = 0$. On the top of the bump C_s is positive, the denominator of Equation (2) is larger, so the removal force is expected to be smaller. On the side of the bump or in a groove C_s is negative, the denominator of Equation (2) is smaller, and there removal force is expected to be larger than it is over flat regions of the surface.

Rough surfaces have a variety of local surface curvatures and the adhesion to different regions on the surface will fluctuate. By measuring adhesion variations, AFM provides a direct test of the validity of the Derjaguin approximation for the surfaces studied here. One can quantify the variation in the removal force by taking the

derivative of Equation (2). One finds that

$$\frac{\delta F_R}{F_R} = \frac{\dfrac{-W\delta C_s}{(C_t + C_s)^2}}{W\left[\dfrac{1}{C_t + C_s}\right]} = R_t \delta C_s \tag{3}$$

By looking at the relative fluctuations in the adhesion rather than the absolute fluctuations, W cancels out of the force expression and one obtains an expression for the adhesion fluctuations which depends only on the geometry of the tip and not at all on the material. The Derjaguin approximation predicts that the relative adhesion fluctuations should be proportional to the surface curvature fluctuations, and the proportionality constant is the radius of curvature of the probe tip.

For rough surfaces, the surface curvature about a point in the two lateral directions can be different and even have opposite signs. When the values are different, the surface about this point is better approximated by an ellipsoid rather than a sphere. However, the Derjaguin approximation cannot be integrated in closed form for an ellipsoid. Equation (3) is then not rigorously correct, but it does give a closed form solution for the variations in adhesion and surface curvature and we use it to explain our experimental results.

The quantities in Equation (3) are available from AFM measurements. The left hand side can be calculated from the adhesion map, and the right hand side from the topography map.

The vertical resolution of the topography map depends on the number of points taken along the loading curve. This resolution is limited by the sensitivity of the analog-to-digital converter in our AFM instrumentation. The resolution can be improved by taking a topography image using the microscope in its original way as a profilometer.[9] Since only variations in the surface topography are being used to test the Derjaguin approximation, the topography at the exact location where the adhesion map was taken is not necessary. We, therefore use profilometer-type images to extract surface curvature variations with high sensitivity.

Figure 6 shows images of surfaces of varying roughnesses. The left images show the topography image of each surface. As in the earlier images, the gray level is proportional to the height of the surface. In this series of images, the proportionality constant is chosen to be the same for the series of four images so one can qualitatively see the increase in surface roughnes. The right four images show the corresponding adhesion maps (not taken over the same areas). The adhesion is also scaled consistently for these four surfaces and the adhesion variations are also seen to increase.

From these images, and a total of 9 others, the adhesion fluctuations and the surface curvature fluctuations were calculated. The adhesion fluctuations were calculated by taking the standard deviations of all adhesion values comprising the adhesion map. The curvature of the topography image was calculated by taking 3 neighboring points in the scan, determining the radius of the circle that runs through these three points, and inverting the circle's radius to get the curvature. The curvature was determined in the scan direction and perpendicular to the scan direction. The curvature was found to

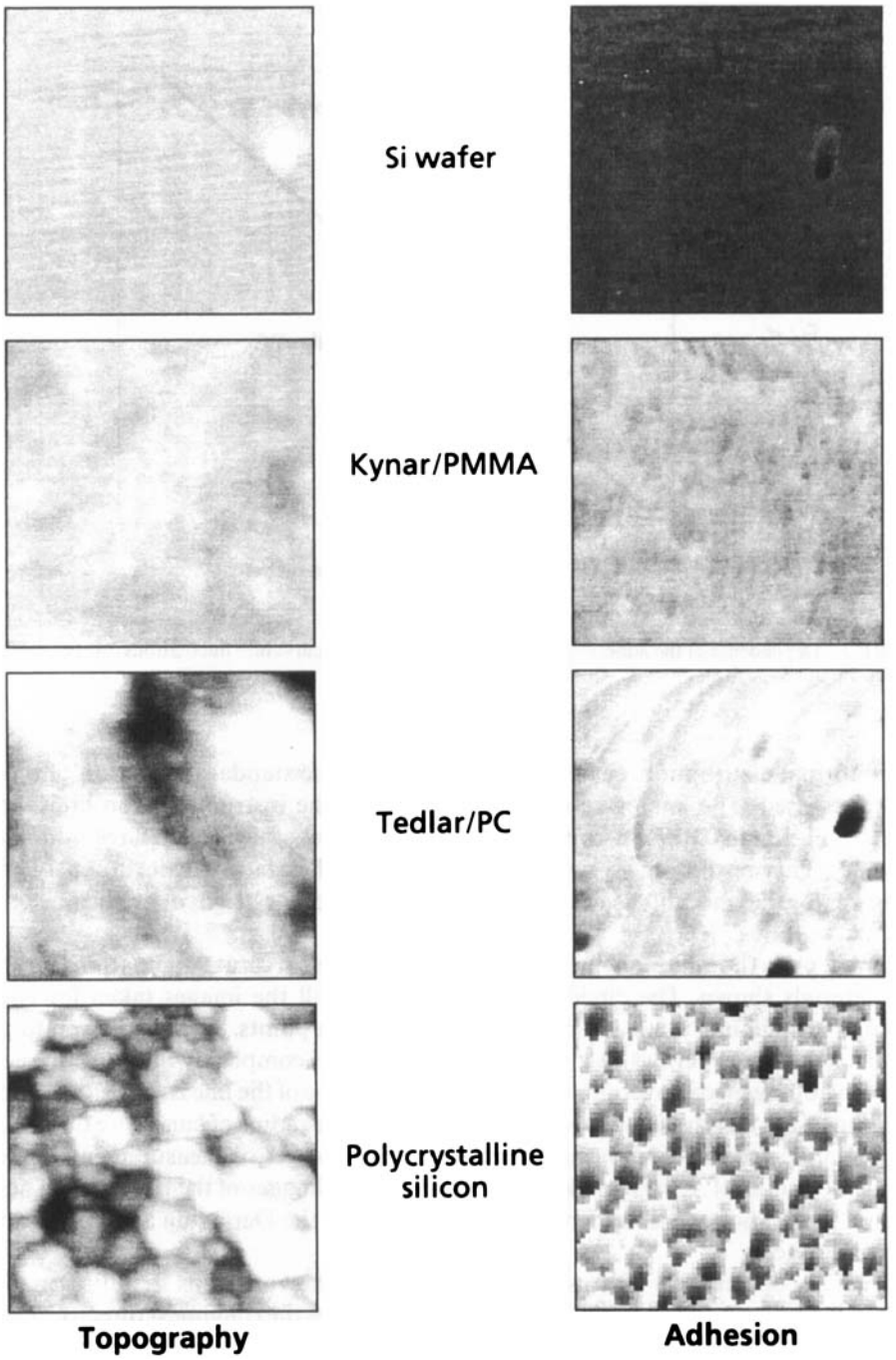

FIGURE 6 (a) Topographic images of Si, Tedlar®/polycarbonate, Kynar®/PMMA, and polysilicon. The correspondence between the gray level and the height of the surface is the same in all the images. The size of both the topography and adhesion maps are $2 \times 2\,\mu m$. The black-to-white height difference is $0.10\,\mu m$. (b) Adhesion maps of Si, Tedlar®/polycarbonate, Kynar®/PMMA, and Polysilicon. The correspondence between the adhesion and the gray scale is the same in all the images, and the black-to-white adhesion difference is the 51 nN.

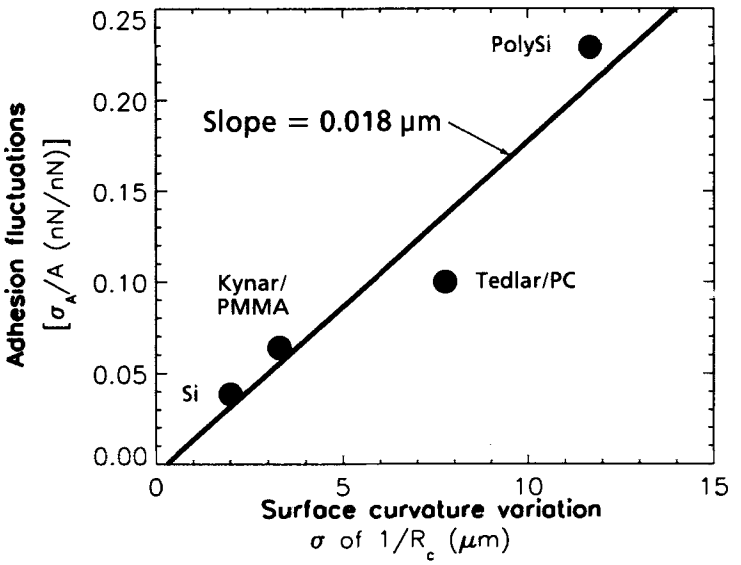

FIGURE 7 Dependence of the adhesion fluctuations on the surface curvature fluctuations for the surfaces shown in Figure 6.

have a normal distribution, centered about zero, and the standard deviation of these values was used. The analog-to-digital converter on the instrumentation limits the height resolution to 0.019 nm, so the curvature can be determined with a resolution of 0.11 μm-1. This resolution is significantly less than the standard deviation of the curvatures for the smoothest surface, so the discretation of the height does not affect the surface curvatures.

Figure 7 plots the adhesion fluctuations *vs.* the surface curvature fluctuations for the four materials shown. The circles are the average of all the images taken for each surface. The solid line is a least squares fit to the 4 data points. The line is seen to go through zero, which verifies that as the surface becomes completely flat the adhesion should be homogeneous over the whole surface. The slope of the line is 0.018 μm, which according to the Derjaguin approximation should be the radius of curvature of the tip. The pyramid tip radius of curvature inferred from these adhesion measurements agrees with the tip radius of < 0.03 μm determined from SEM images of the pyramid.[7] These adhesion fluctuation measurements give a direct test of the Derjaguin approximation for these surfaces.

Intuitively, one expects that as a surface roughens the variations in adhesion will increase. However, we wish to emphasize here that it is not the roughness directly that is driving the adhesion fluctuations, but the variations in surface curvature. If the RMS surface roughness is extracted from the data in Figure 6, one gets erroneous results. The RMS roughness of the polysilicon surface is 0.21 μm, larger than the 0.14 μm RMS roughness of the Tedlar®/polycarbonate surface. However, as seen in Figure 7, the polysilicon adhesion fluctuations are 0.23 nN/nN, over twice as large as the 0.10 nN/nN measured for Tedlar®/polycarbonate. The measured RMS roughnesses of the

silicon wafer and Kynar®/PMMA are 0.007 μm and 0.34 μm, respectively. If one fits a straight line to the RMS roughness data, then one finds that for zero RMS roughness the adhesion fluctuations are an unreasonable 0.06 nN/nN when they should be zero. The explanation for these discrepancies is that it is not only the surface roughness that drives adhesion variations, but also the length scale over which it occurs, and these effects are embodied in using the surface curvature.

6. CONCLUSIONS

The work described here shows that the atomic force microscope is a powerful tool to measure adhesion inhomogeneities with high resolution and sensitivity. The ability to make these measurements allows for improvement in the xerographic process, where particles must be moved controllably from one surface to another. However, these types of measurements can also be applied to thin film adhesion, where surface inhomogeneities might provide a weak point where film adhesion would first fail.

Adhesion maps were used to quantify how surface roughness can change particle adhesion. Comparison of adhesion maps and topography maps shows directly that there is a topographic dependence of adhesion and that it dominates the adhesion for the surfaces presented here. In addition, variations in the surface roughness give rise to variations in the adhesion. These variations can be used to verify the Derjaguin approximation directly, which implies that the forces driving the adhesion for these particles are long range.

References

1. L. B. Schein, *Electrophotography and Development Physics* (Springer, New York, 1988).
2. M. Scharfe, *Electrophotography Principles and Optimization* (Wiley, New York, 1984).
3. H. A. Mizes, *J. Adhesion Sci. Technol.* **8**, 937 (1994).
4. H. A. Mizes, K.-G. Loh, R. J. D. Miller, S. K. Ahuja and E. F. Grabowski, *Appl. Phys. Lett.* **59**, 2901 (1991).
5. G. Meyer and N. M. Amer, *Appl. Phys. Lett.* **56**, 2100 (1990).
6. D. M. Schaefer, M. Carpenter, B. Gady, R. Reifenberger, L. P. DeMejo and D. S. Rimai, to be published in *J. Adhesion Sci. Technol.*
7. T. R. Albrecht, S. Akamine, T. E. Carver, and C. F. Quae, *J. Vac. sci. Technol.* **A8**, 3386 (1990).
8. J. N. Israelachvili, *Intermolecular and Surface Forces* (Academic Press, London, 1985), p. 130–133.
9. D. Rugar and P. Hansma, *Physics Today*, October 1990, p. 23–30.